

Temperature-based Instanton Analysis: Identifying Vulnerability in Transmission Networks

Jonas Kersulis,
Ian Hiskens
Elec. Eng. and Computer Science
University of Michigan
Ann Arbor, MI, United States

Michael Chertkov,
Scott Backhaus
Center for Nonlinear Studies
Los Alamos National Laboratory
Los Alamos, NM, United States

Daniel Bienstock
Ind. Eng. and Operations Research
Columbia University
New York, NY, United States

Abstract—A time-coupled instanton method for characterizing transmission network vulnerability to wind generation fluctuation is presented. To extend prior instanton work to multiple-time-step analysis, line constraints are specified in terms of temperature rather than current. An optimization formulation has been developed that determines the minimum deviation in wind power from the forecast such that line temperature is driven to its limit. Results are shown for an IEEE RTS-96 system with several wind farms.

Index Terms—Forecast uncertainty, Optimization, Transmission operations, Wind energy

I. INTRODUCTION

The prevalence of renewables in modern transmission networks has researchers and system operators asking: What happens when the wind changes, and could fluctuations harm the grid? The instanton problem provides an answer, and this paper extends instanton analysis to the temporal setting. Though small deviations from wind forecasts are typically harmless, it is possible for certain wind generation patterns to drive the system to an infeasible operating point. Out of all troublesome wind generation patterns, the one that deviates least from the forecast is called the instanton. Instanton analysis uses optimization to find the set of troublesome wind patterns (each of which is guaranteed to cause a particular line to encounter its current flow limit). By ranking these wind patterns according to distance from forecast, we can characterize the system's vulnerability to forecast inaccuracy and enable system operators to prepare in advance.

Previous work has solved several variants of the instanton problem. In 2012 [1] used the physically accurate AC power flow equations and found instanton candidates with an iterative scheme. Other papers, including [2] and [3], have used the DC power flow approximation to turn instanton analysis into a convex problem with an analytic solution. Current instanton research is exploring the trade-off between problem complexity and solution accuracy, with the goal of developing the most accurate model that remains convex (and therefore guarantees a solution). To the authors' knowledge, all instanton work to date has focused on instantaneous vulnerability. In other words, prior work has assumed fixed demand and generator

dispatch, and has used power or current limits as constraints. Thus, the troublesome wind patterns uncovered by instanton analysis may be fleeting.

It is safe to temporarily operate a line above its current limit. Transmission system operators know this and periodically allow lines to operate above their limits to promote smooth operation under heavy load (see the introduction of [4] for a history of dynamic line rating starting in the 1970s). It takes time for a line to accumulate enough heat to cause it to sag to an unacceptable level (as defined by statute and nearby tree limbs). As long as the line is allowed to cool before reaching this point, no harm will be done. If an operator is comfortable with temporarily overloaded lines, information from today's instanton analysis may be too conservative to aid in decision making.

In this paper we bring instanton analysis into the temporal setting. We consider multiple time steps and replace line current limits with heat constraints. A line's temperature change is a function of heat input (primarily Ohmic losses and heat from the sun) and dissipation (convection and radiation, which depend on ambient conditions), and is represented as a differential equation (see Section 3.4 of [5] for a standard set of equations governing line temperature dynamics). Ohmic loss heating is proportional to the square of current, and dissipation is related primarily to ambient temperature and wind speed. By modeling line temperature over a significant time horizon, the new method discovers multiple-time-step wind patterns that are both likely to occur and sure to induce excessive sagging for at least one line in the network.

II. PROBLEM FORMULATION

Though most of the modeling and detail of previous instanton work carries over to time-coupled analysis, there is one significant complication: the nonlinearity of Ohmic heating (power loss) on a line. Heat input into a line is proportional to the square of the line's current. Thus, heat-constrained, time-coupled instanton analysis is a quadratically-constrained quadratic program (QCQP). QCQPs are NP-hard in general; reasonable solutions may exist, but unless the quadratic constraint matrices are positive-definite there is no solution guarantee (see [6]). Because system operators must be able to reliably obtain reasonable output from the analysis, "no

The authors acknowledge the support of the Los Alamos National Laboratory Grid Science Program, subcontract 270958.

TABLE I
LINE HEATING PARAMETERS

Parameter	Units	Description
T_s	s	Sample time
mC_p	$J/(m \cdot C)$	Per-unit-length heat capacity of the conductor
η_c	$W/(m \cdot C)$	Conductive heat loss rate coefficient
η_r	$W/(m \cdot C)$	Radiative heat loss rate coefficient
T^{lim}	C	Line temperature at steady-state current limit.
$\Delta q_{s,ij}$	W/m	Solar heat input into conductor
ΔT_{amb}	C	Change in ambient temperature

solution found” is an unacceptable output. With this criterion in mind, we proceed to develop models for line losses, line temperature, and instanton optimization that keep problem complexity to a minimum.

A. Line losses

Starting with the AC line loss expression, [7] derived the following approximate relationship between line losses and voltage angle differences:

$$f_{ij}^{\text{loss}} \approx r_{ij} \left(\frac{\theta_{ij}}{x_{ij}} \right)^2 \quad (1)$$

where f_{ij} is the active power flow from node i to node j . This expression is predicated on three assumptions: voltage magnitudes are all 1 pu, cosine may be approximated by its second-order Taylor expansion, and $x_{ij} \geq 4r_{ij}$ (line reactance is at least four times as great as resistance). Equation (1) simplifies the full AC line loss formulation using DC assumptions, but remains nonlinear.

B. Line temperature dynamics

According to analysis done in [7] (which is based on [5]), changes in line temperature may be calculated using the following Euler integration:

$$\Delta T_{ij}[t+1] = \tau_{ij} \Delta T_{ij}[t] + \rho_{ij} \Delta f_{ij}^{\text{loss}}[t] + \delta_{ij} \Delta d_{ij}[t], \quad (2)$$

where the initial condition is $\Delta T_{ij}[0] = 0$. τ_{ij} and $\bar{\gamma}_c$ are defined as

$$\tau_{ij} = 1 - \frac{T_s \bar{\gamma}_c}{mC_p}, \quad \bar{\gamma}_c = \eta_c + 4\eta_r (T^{\text{lim}} + 273)^3, \quad (3)$$

and $\rho_{ij} = T_s/mC_p$. Finally, $\Delta d_{ij} = \text{col}(\Delta q_{s,ij}, \Delta T_{\text{amb}})$, and δ_{ij} represents exogenous inputs and is equal to $[\rho_{ij} \ \bar{\gamma}_{ij}]$, where

$$\bar{\gamma}_{ij} = \frac{T_s \bar{\gamma}_a}{mC_p}, \quad \bar{\gamma}_a = \eta_c + 4\eta_r (T_{\text{amb}}^* + 273)^3. \quad (4)$$

The parameters in this line temperature model are described in Table I.

For numerical stability, we need $\tau_{ij} \in (-1, 1)$, which leads to the following constraint on sampling time for the integration:

$$T_s < \min_{ij} \left\{ \frac{2mC_{p,ij}}{\bar{\gamma}_{c,ij}} \right\} \quad (5)$$

Having introduced the necessary equations for modeling line temperature, we now recognize (2) as a relationship between angle differences and constants. Note that (2) is a recursive relationship between temperature at time $t+1$ and temperature at time t . Repeatedly substituting into this equation and using (1), we find the following expression for change in line temperature at time t^* :

$$\begin{aligned} \Delta T_{ik}[t^*] &= \frac{\rho_{ik} r_{ik}}{x_{ik}^2} \sum_{t=1}^{t^*} \tau_{ik}^{t-1} \theta_{ik}^2[t^* - t] + \\ &+ \delta_{ik} \sum_{t=1}^{t^*} \tau_{ik}^{t-1} \Delta d_{ik}[t^* - t] \end{aligned} \quad (6)$$

The first term in Equation (6) varies with angle differences. The second term, which is based on external conditions, is constant with respect to all power flow variables. Moving all constants to the left-hand side, we find:

$$\begin{aligned} \Delta T_{ik}[t^*] - \delta_{ik} \sum_{t=1}^{t^*} \tau_{ik}^{t-1} \Delta d_{ik}[t^* - t] &= \\ &= \frac{\rho_{ik} r_{ik}}{x_{ik}^2} \sum_{t=1}^{t^*} \tau_{ik}^{t-1} \theta_{ik}^2[t^* - t] \end{aligned} \quad (7)$$

The left side of (7) is constant during optimization, and the right side is a weighted, scaled two-norm of the vector of angle difference variables $\theta_{ik}[t]$, $t \in \{1, \dots, t^*\}$. Now we define

$$\boldsymbol{\theta}_{ik} := [\theta_{ik}[0]^2 \ \theta_{ik}[1]^2 \ \dots \ \theta_{ik}[t^* - 1]^2]^\top \quad (8)$$

$$\boldsymbol{\tau}_{ik} := [\tau_{ik}^{t^*-1} \ \tau_{ik}^{t^*-2} \ \dots \ 1]^\top \quad (9)$$

$$\boldsymbol{\Delta d}_{ik} := [\Delta d_{ik}[0] \ \Delta d_{ik}[1] \ \dots \ \Delta d_{ik}[t^* - 1]]^\top \quad (10)$$

Note that these three vectors are implicit functions of t^* , but this dependence is hidden in their notation to promote conciseness. Having defined these three vectors, we can express (7) as follows:

$$\Delta T_{ik}[t^*] - \delta_{ik} \boldsymbol{\tau}_{ik}^\top \boldsymbol{\Delta d}_{ik} = \frac{\rho_{ik} r_{ik}}{x_{ik}^2} \boldsymbol{\tau}_{ik}^\top \boldsymbol{\theta}_{ik} \quad (11)$$

The temperature dynamics described in this section are used in the following development of the instanton formulation itself.

C. Instanton formulation

In the preceding discussion we have shown how to calculate losses with (1) and use this information to find line temperature changes with (2)-(5) and ultimately (11). All that remains is to describe the instanton optimization itself.

The following equations describe an optimization problem that minimizes deviation from the wind forecast while heating a certain line to an unacceptable temperature by the last time step:

$$\min \sum_{t=1}^{t_{\text{end}}} x_t^\top Q_x x_t \quad (12a)$$

subject to:

$$\sum_k Y_{ik} \theta_{ik,t} = G_{i,t} + \rho_{i,t} + x_{i,t} - D_{i,t} \quad \forall i \in \mathcal{N}, t \in 1 \dots T \quad (12b)$$

$$G_t = G_{0,t} + k \alpha_t \quad \forall t \in 1 \dots T \quad (12c)$$

$$\theta_{k,t} = 0 \quad \forall t \in 1 \dots T \quad (12d)$$

$$\Delta T_{ik}[T] = \Delta T_{ik}^{\text{lim}} \quad \text{for some } (i, k) \in \mathcal{G} \quad (12e)$$

together with (1) and (2), where:

- $x_{i,t}$ is the difference between actual output and forecast output at wind farm i and time t . Thus, x is a vector of wind forecast deviations.
- Q_x may be set to the identity matrix or used to encode correlation between wind sites.
- $\rho_{i,t}$ is renewable generation forecast at bus i and time t in per unit
- Y_{ik} is the (i, k) -th element of the admittance matrix Y , which assumes resistances throughout the network are zero.
- $\theta_{ik,t}$ is the difference between the bus i phase angle and the bus k phase angle at time t .
- $G_{i,t}$ is the conventional active power generation at node i and time t .
- $D_{i,t}$ is the active power demand at bus i and time t .
- \mathcal{N} is the set of buses (nodes).
- G_t is the vector of conventional active power generation at time t .
- $G_{0,t}$ is the scheduled conventional active power generation (without droop response).
- k is the vector of participation factors for conventional generators, with

$$\sum_i k_i = 1. \quad (13)$$

The case where $k_i = 1$ corresponds to generator i taking up all slack.

- α_t is the participation coefficient (mismatch) at time t , defined as

$$\alpha_t := \sum D_t - \sum \rho_t - \sum G_{0,t}.$$

- $\Delta T_{ik}^{\text{lim}}$ is the change in temperature that will push line (i, k) to its thermal limit.
- θ_{ref} is the phase angle of the reference bus (fixed at zero).
- \mathcal{G} is the set of edges (lines).

Equation (12a) expresses the desire to find wind patterns that remain close to the wind forecast. The first constraint

equation (12b) enforces DC power balance. The next constraint (12c) models conventional active power generation as a sum of scheduled generation and droop response (where generators share the task of compensating for mismatch between total generation and total load). The system angle reference is established by (12d). Last is (12e), which constrains the temperature of a particular line to be equal to its limit at the final time t_{end} . By (11), we can express (12e) as

$$\Delta T_{ik}[T] - \delta_{ik} \tau_{ik}^\top \Delta \mathbf{d}_{ik} = \frac{\rho_{ik} r_{ik}}{x_{ik}^2} \tau_{ik}^\top \boldsymbol{\theta}_{ik}. \quad (14)$$

Because the slack bus is specified to be bus k in (12d), (12e) may be viewed as an equality constraint on the vector of squared angle variables $\theta_i[t]^2$, $t \in \{0, 1, \dots, t_{\text{end}}\}$. Thus, (12) has a quadratic objective function, a set of linear constraints, and a single quadratic constraint.

By solving (12) for each line $(i, k) \in \mathcal{G}$, we obtain a set of instanton candidate wind patterns, each of which will heat a particular line to its thermal limit. Of these candidates, the one that deviates least from the wind forecast (across all time steps) is the instanton wind pattern.

III. CONVERSION TO OPTIMIZATION PROBLEM

If we arrange all variables into a single vector, (12) may be viewed as a quadratically-constrained quadratic program (QCQP) of the following form:

$$\min z^\top Q_{\text{obj}} z \quad (15a)$$

$$s.t. \quad Az = b \quad (15b)$$

$$z^\top Q_\theta z = c \quad (15c)$$

The objective (15a) is equivalent to (12a), the linear equality constraints (15b) represent (12b)-(12d), and the quadratic equality constraint (15c) is equivalent to (12e). z consists of $(n + n_r + 1)t^*$ variables, where n is the number of nodes, n_r is the number of nodes with wind farms, and t^* is the number of time steps.

- $n_r t^*$ of these are deviation variables,
- $(n - 1)t^*$ are angle variables,
- t^* are mismatch variables (one per time step), and
- t^* are angle difference variables $\hat{\theta}_{ik}$ representing the difference between θ_i and θ_k at each time step. These variables are used to convert the quadratic constraint into a norm constraint.

Thus, the vector z consists of t^* groups of $(n + n_r)$ variables stacked together (one for each time step), with a set of t^* angle difference variables at the end. At a particular time step t , the group of variables is $[x_t^\top \theta_t^\top \alpha_t]^\top$. x_t represents deviations from forecast at the n_r wind nodes, θ_t is the column of $n - 1$ independent angle variables at time t , and α_t is the mismatch between generation and demand at time t . An instance of the temporal instanton problem is characterized by Q_{obj} , A , b , and Q_θ . Following is a description of each part.

A. Objective function and Q_{obj}

The objective function depends solely on deviation variables x , so Q_{obj} is a matrix that weights only the x variables in z . If there are two time steps, for example, the vector of variables would be $z = [x_t^\top \ \theta_1^\top \ \alpha_1 \ x_2^\top \ \theta_2^\top \ \alpha_2 \ \hat{\theta}]^\top$, and Q_{obj} would be

$$Q_{obj} = \begin{bmatrix} Q_x & 0 & 0 & 0 & 0 & 0 \\ 0 & 0 & 0 & 0 & 0 & 0 \\ 0 & 0 & 0 & 0 & 0 & 0 \\ 0 & 0 & 0 & Q_x & 0 & 0 \\ 0 & 0 & 0 & 0 & 0 & 0 \\ 0 & 0 & 0 & 0 & 0 & 0 \end{bmatrix},$$

where Q_x represents the correlation between wind farms (if any). In our RTS-96 analysis later on, we will assume $Q_x = I$, the identity matrix.

B. Linear constraints: A and b

All constraints except the temperature limit may be grouped into a single linear equation $Az = b$. Setting aside the $\hat{\theta}_{ik}$ angle difference variables for the moment, the A matrix has a block diagonal structure where each block consists of $(n+1)$ rows and $(n_r + n)$ columns. The first n rows describe power balance and distributed slack behavior. We have the following equation for a non-slack node with a wind farm (with all variables on the left-hand side and constants on the right):

$$-x_{i,t} + \sum_{k \neq s} Y_{ik} \theta_{k,t} - k_i \alpha_{i,t} = G_{i,t}^0 + \rho_{i,t} - D_{i,t},$$

where the slack node is node s . Rearranging, we see that this equation is simply power balance in disguise:

$$\sum_{k \neq s} Y_{ik} \theta_{k,t} = (G_{i,t}^0 + k_i \alpha_t) + (\rho_{i,t} + x_{i,t}) - D_{i,t} \quad (16)$$

The first pair of terms on the right-hand side of (16) represents conventional generation with distributed slack – generator i is taking a portion k_i of the mismatch α_t . The second pair of terms is renewable generation: forecast $\rho_{i,t}$ plus deviation $x_{i,t}$. The final term is demand at node i and time t . For a non-slack node with a wind farm, the equation is (16) without the renewable generation terms. For a slack node, we have (16) with the left-hand side equal to 0 (keeping track of distributed slack only). In addition to the n rows corresponding to (16) at the n nodes, there is one additional equation used to fix α_t (again, with variables on the left and constants on the right):

$$\sum_i x_{i,t} + \alpha_t = \sum_i (D_{i,t} - G_{i,t}^0 - \rho_{i,t})$$

Rearranging, we see that this simply fixes α_t to the difference between generation and demand at time t :

$$\alpha_t = \sum_i (D_{i,t} - G_{i,t}^0 - (\rho_{i,t} + x_{i,t})) \quad (17)$$

From (17) we see that α_t is positive when demand exceeds generation. This causes conventional generators to increase their output according to (12c).

The previously described $(n+1)$ rows of $Az = b$ pertain to a single time step block. The T total blocks are arranged diagonally to form $(n+1)T$ rows of A . There is one additional block of A used to relate angle difference variables $\hat{\theta}_{ik}$ to angle variables θ_i and θ_k . This block contains one row for each time step. At time t , we have:

$$\hat{\theta}_{ik,t} = \tau^{\frac{t^* - t}{2}} (\theta_{i,t} - \theta_{k,t}) \quad (18)$$

Equivalence of this relationship to (14) is discussed in the next subsection.

C. Quadratic constraint: $Q_{\hat{\theta}}$ and c

Recall that (14) describes the temperature constraint on a chosen line (i, k) . The only variable component of the relationship is θ_{ik} , so we can express (14) with a constant on the right-hand side that represents known ambient conditions and line parameters:

$$\sum_{t=1}^{t^*} \tau_{ik}^{t^* - t} (\theta_{i,t} - \theta_{k,t})^2 = \frac{x_{ik}^2}{\rho_{ik} r_{ik}} (\Delta T_{ik}^{lim} - \delta_{ik} \tau_{ik}^\top \Delta \mathbf{d}_{ik}) \quad (19)$$

From the definition of $\hat{\theta}_{ik,t}$ in (18), we see that (19) may be expressed as:

$$\sum_{t=1}^{t^*} \hat{\theta}_{ik,t}^2 = \frac{x_{ik}^2}{\rho_{ik} r_{ik}} (\Delta T_{ik}^{lim} - \delta_{ik} \tau_{ik}^\top \Delta \mathbf{d}_{ik}) \quad (20)$$

With $\hat{\theta}_{ik}$ as the last t^* elements of z , we see that the matrix $Q_{\hat{\theta}}$ in (15c) is a matrix of zeros with a t^* -by- t^* identity matrix in the lower-right corner. In other words, our temperature constraint becomes

$$\|\hat{\theta}_{ik}\|^2 = c^2,$$

where

$$c = \frac{x_{ik}^2}{\rho_{ik} r_{ik}} (\Delta T_{ik}^{lim} - \delta_{ik} \tau_{ik}^\top \Delta \mathbf{d}_{ik}).$$

IV. SOLUTION

The structure of (15) is similar to that of the well-known trust-region subproblem. Here we describe a four-step solution method based in part on work from [8]. We begin by considering the vector of variables z as three groups: $z_1 \in \mathbb{R}^{N_r T}$ contains wind deviations, $z_2 \in \mathbb{R}^{(N+1)T}$ contains angle and mismatch variables, and $z_3 \in \mathbb{R}^T$ contains angle difference variables involved in line temperature calculation. With this notation, the problem becomes

$$\begin{aligned}
& \min z_1^\top Q_z z_1 \\
s.t. \quad & Az = b \\
& z_3^\top z_3 = c
\end{aligned}$$

where Q_z encodes wind correlation, if any.

A. Translation

The first step is to translate the problem to change the form of the linear constraints from $Az = b$ to $Ay = 0$. This is equivalent to a change of variables where $y = z - z^*$ and $z^* \in \{z : Az = b\}$ is the translation. Because translation must not introduce a linear term into the quadratic constraint, z_3^* must be zero. To satisfy $Az^* = b$, then, z_1^* and z_2^* must satisfy

$$A \begin{bmatrix} z_1^* \\ z_2^* \\ 0 \end{bmatrix} = b.$$

It is straightforward to find a min-norm z^* that satisfies this constraint.

After translation, the problem takes the form

$$\min y_1^\top Q_z y_1 + 2y_1^\top Q_z z_1^* \quad (21a)$$

$$s.t. \quad Ay = 0 \quad (21b)$$

$$y_3^\top y_3 = c \quad (21c)$$

B. Kernel mapping

The new form of the linear constraints suggests an intuitive explanation: any solution to (21) must lie in the nullspace (kernel) of A . If $\dim \mathcal{N}(A) = k$ is the dimension of this nullspace, we can replace y by Nx where $N \in \mathbb{R}^{n \times k}$ spans $\mathcal{N}(A)$. This change of variables is somewhat similar to a rotation, but it reduces the problem dimension to k . It also ensures that feasible solutions x to the new problem lie in the nullspace of A , as required. After the change of variables, the problem becomes

$$\min x^\top (N^\top Q_{obj} N) x + 2x^\top N^\top (Q_z z_1^*) \quad (22a)$$

$$s.t. \quad x^\top N_3^\top N_3 x = c, \quad (22b)$$

where the linear constraints are implicit.

C. Obtaining a norm constraint

After kernel mapping, the quadratic constraint is no longer diagonal. We can fix this by performing an Eigendecomposition $N_3^\top N_3 = UDU^\top$ and letting $\hat{x} = U^\top x$. The constraint becomes diagonal when expressed in terms of \hat{x} :

$$x^\top N_3^\top N_3 x = \hat{x}^\top D \hat{x} \quad (23)$$

In this new constraint expression, D is diagonal and has at most T nonzero elements. It will look like this:

$$D = \begin{bmatrix} 0 & 0 \\ 0 & \hat{D} \end{bmatrix} \quad (24)$$

The quadratic constraint (23) is diagonal, but one more change of variables can render it a norm constraint. Let $\hat{x} = [\hat{x}_1 \ \hat{x}_2]^\top$ and $w = [w_1 \ w_2]^\top$, and relate them as follows:

$$\begin{aligned}
\begin{bmatrix} w_1 \\ w_2 \end{bmatrix} &= \begin{bmatrix} I & 0 \\ 0 & \hat{D}^{1/2} \end{bmatrix} \begin{bmatrix} \hat{x}_1 \\ \hat{x}_2 \end{bmatrix} = K \hat{x} \\
\implies w &= KU^\top x
\end{aligned} \quad (25)$$

Using (25) we can rewrite the constraint in terms of w :

$$\hat{x}^\top D \hat{x} = \hat{x}_2^\top \hat{D}^{1/2} \hat{D}^{1/2} \hat{x}_2 = w_2^\top w_2 \quad (26)$$

(Note that $z = UK^{-1}w$ because $UU^\top = I$. Changing from z to w is equivalent to rotating by $(UK^{-1})^\top$.)

This change of variables also influences the cost function. After substitution and simplification, the optimization problem becomes

$$\min w^\top B w + w^\top b \quad (27a)$$

$$s.t. \quad w_2^\top w_2 = c \quad (27b)$$

where

$$B = K^{-1}U^\top N^\top Q_z N U K^{-1} \text{ and } b = 2K^{-1}U^\top N_1 z_1^*.$$

The purpose of this section was to change variables to obtain a norm constraint. The next section eliminates w_1 using the KKT conditions of (27). This will allow us to write the objective in terms of w_2 only.

D. Eliminating w_1

Note that w_1 is unconstrained in (27). For a fixed w_2 , we can use the KKT conditions to find w_1 such that the objective is minimized. Begin by expanding the objective:

$$\begin{aligned}
f(w) &= [w_1^\top \ w_2^\top] \begin{bmatrix} B_{11} & B_{12} \\ B_{12}^\top & B_{22} \end{bmatrix} \begin{bmatrix} w_1 \\ w_2 \end{bmatrix} + [w_1^\top \ w_2^\top] \begin{bmatrix} b_1 \\ b_2 \end{bmatrix} \\
&= w_1^\top B_{11} w_1 + 2w_1^\top B_{12} w_2 + w_2^\top B_{22} w_2 + w_1^\top b_1 + w_2^\top b_2
\end{aligned}$$

Set the partial derivative with respect to w_1 equal to zero:

$$\begin{aligned}
\frac{\partial f}{\partial w_1} &= 2w_1^\top B_{11} + 2w_2^\top B_{12}^\top + b_1^\top = 0 \\
\iff w_1 &= -B_{11}^{-1} \left(B_{12} w_2 - \frac{1}{2} b_1 \right) \quad (28)
\end{aligned}$$

After substitution and simplification, the objective depends on w_2 only:

$$\begin{aligned}
f(w_2) &= w_2^\top (B_{22} - B_{12}^\top B_{11}^{-1} B_{12}) w_2 + w_2^\top (b_2 - B_{12}^\top B_{11}^{-1} b_1) \\
&\quad - \frac{1}{4} b_1^\top B_{11}^{-1} b_1
\end{aligned}$$

(Note that the last term is constant and therefore plays no role in the minimization.) The optimization problem in terms of w_2 is:

$$\min w_2^\top \hat{B} w_2 + w_2^\top \hat{b} \quad (29a)$$

$$s.t. \quad w_2^\top w_2 = c \quad (29b)$$

where

$$\hat{B} = B_{22} - B_{12}^\top B_{11}^{-1} B_{12} \text{ and } \hat{b} = b_2 - B_{12}^\top B_{11}^{-1} b_1.$$

In (29) the goal is to minimize a T -dimensional quadratic objective subject to a T -dimensional norm constraint.

E. Solution via enumeration

Let v be the Lagrange multiplier associated with the constraint. Then the following is a first-order optimality condition for (29):

$$\begin{aligned} \frac{\partial \mathcal{L}(w_2, v)}{\partial w_2} &= 2\hat{B}w_2 + \hat{b} - v(2w_2) = 0 \\ \implies \hat{B}w_2 + \frac{1}{2}\hat{b} &= vw_2 \end{aligned} \quad (30)$$

The above expression is a linear system that yields each element of w_2 when v is fixed:

$$w_{2,i} = \frac{\hat{b}_i/2}{v - \hat{B}_{i,i}} \quad (31)$$

In addition to satisfying (31), an optimal w_2 must satisfy the quadratic constraint. Substituting (31) into (29b) yields the “secular equation” (see [8]):

$$s(v) = \sum_i \left(\frac{\hat{b}_i/2}{v - \hat{B}_{i,i}} \right)^2 = c \quad (32)$$

The secular equation has one pole per unique non-zero diagonal element of \hat{B} . There are at most two solutions per pole: one to the left and the other to the right. This is best understood graphically. Below we have a secular equation with one pole, taken from analysis of the RTS-96 network. The horizontal axis is the value of the Lagrange multiplier v , and the vertical axis is $s(v)$, the value of the secular equation. The horizontal line is $s(v) = c$. The two intersection points are the two solutions to this secular equation.

V. RESULTS FOR RTS-96 NETWORK

We used data from a wind-augmented RTS-96 ?? to illustrate temporal instanton analysis. Consider a scenario unfolding over three time steps: in the first time step, the wind forecast is scaled to one-half its value at the second time step. In the third step, the wind forecast is scaled to 1.5 times its value at the second time step. Generator dispatch and demand remain constant during this period. Temporal instanton analysis with $c = 0.1$ and $\tau = 1$ indicates that the line from bus 56 to bus 57 is most susceptible to excessive heating. In other words,

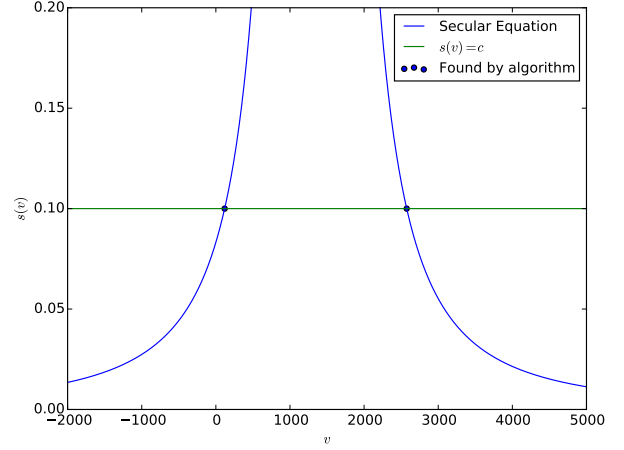


Fig. 1. Plot of secular equation for a single line in the RTS-96. Note that $s(v)$ approaches infinity at the pole.

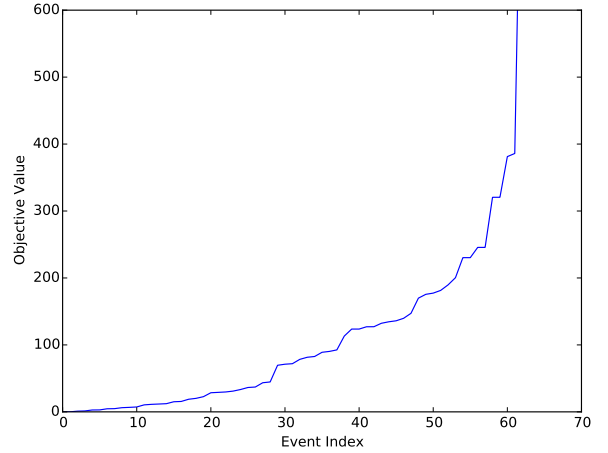


Fig. 2. Plot of sorted objective values for 63 lines from RTS-96 temporal instanton analysis.

of all dangerous wind patterns (patterns that cause a line to overheat), the most likely to occur is a pattern that overheats the line from bus 56 to bus 57. We call this the instanton wind pattern. The secular equation used to find this pattern is shown in Figure 1.

The largest deviation in the instanton pattern is 0.38 pu, well within the range of wind forecast values (whose maximum is 1.2 pu). Because instanton analysis finds a set of wind patterns and objective values, sorting provides a powerful way to characterize the potential effects of wind disturbances. Figure (2) illustrates a sharp increase in objective value roughly halfway through the set of sorted events (after 60 of the 120 lines).

REFERENCES

- [1] S. Bagsorkhi and I. Hiskens, “Analysis tools for assessing the impact of wind power on weak grids,” in *Proc. Systems Conference (SysCon)*,

- 2012 *IEEE International*, 2012, pp. 1–8.
- [2] M. Chertkov, F. Pan, and M. Stepanov, “Predicting failures in power grids: The case of static overloads,” *IEEE Transactions on Smart Grid*, vol. 2, no. 1, pp. 162–172, Mar. 2011.
 - [3] M. Chertkov, M. Stepanov, F. Pan, and R. Baldick, “Exact and efficient algorithm to discover extreme stochastic events in wind generation over transmission power grids,” in *Proc. 2011 50th IEEE Conference on Decision and Control and European Control Conference (CDC-ECC)*, 2011, pp. 2174–2180.
 - [4] H. Banakar, N. Alguacil, and F. Galiana, “Electrothermal coordination part I: theory and implementation schemes,” *IEEE Transactions on Power Systems*, vol. 20, no. 2, pp. 798–805, May 2005.
 - [5] “IEEE standard for calculating the current-temperature of bare overhead conductors,” *IEEE Std 738-2006 (Revision of IEEE Std 738-1993)*, pp. c1–59, Jan. 2007.
 - [6] O. Mehanna, K. Huang, B. Gopalakrishnan, A. Konar, and N. Sidiropoulos, “Feasible point pursuit and successive approximation of non-convex QCQPs,” *IEEE Signal Processing Letters*, vol. PP, no. 99, pp. 1–1, 2014.
 - [7] M. Almassalkhi and I. Hiskens, “Model-predictive cascade mitigation in electric power systems with storage and renewables – part I: Theory and implementation,” *IEEE Transactions on Power Systems*, vol. PP, no. 99, pp. 1–11, 2014.
 - [8] D. Bienstock and A. Michalka, “Polynomial Solvability of Variants of the Trust-region Subproblem,” in *Proceedings of the Twenty-Fifth Annual ACM-SIAM Symposium on Discrete Algorithms*, ser. SODA ’14. Portland, Oregon: SIAM, 2014, pp. 380–390. [Online]. Available: <http://dl.acm.org/citation.cfm?id=2634074.2634102>